

# Seismic Risk Assessment of Italian School Buildings

Barbara Borzi, Paola Ceresa, Marta Faravelli, Emilia Fiorini,  
and Mauro Onida

**Abstract** Most of the Italian school buildings were not designed according to seismic criteria and, therefore, they are vulnerable from a seismic point of view. A clear proof of this was the catastrophic collapse of the school at San Giuliano during the October 2002 earthquake: thirty people died, of which twenty seven were young students and one their teacher. After this seismic event, the process for identifying the most seismically vulnerable school buildings was started in Italy, with the final aim of improving their strength. Furthermore, several school buildings, mainly located in the historical town centre were damaged during the recent seismic event of L'Aquila (April 6, 2009), as reported by Salvatore et al. (Rapporto dei danni provocati dall'evento sismico del 6 aprile sugli edifici scolastici del centro storico de L'Aquila, <http://www.reluis.it>). The proposed research work was driven by the idea of defining a methodology that implements an analysis in successive steps with an increasing level of detail. Only the buildings with seismic risk higher than a given threshold go through to the following phase, so that the number of buildings analysed decreases at each phase. The implemented procedure follows some well known works published in literature (Grant et al. 2007; Crowley et al. 2008). The definition of a prioritisation scheme of intervention is strictly due to the high number of school buildings (almost 50000) that cannot be deeply analysed considering the limited resources available. The school building location, the exposure data and seismic input information are implemented in a WebGIS platform through interactive maps and tabs. By means of the developed WebGIS tools, the seismic risk analyses of the school buildings are performed and the obtained results, in terms of maps and tables, are herein presented.

**Keywords** Seismic risk · School buildings · Vulnerability · Conventional resistance

---

B. Borzi · P. Ceresa · M. Faravelli (✉) · E. Fiorini · M. Onida  
European Centre for Training and Research in Earthquake Engineering (EUCENTRE),  
Via Ferrata 1, 27100 Pavia, Italy  
e-mail: [marta.faravelli@eucentre.it](mailto:marta.faravelli@eucentre.it)

P. Ceresa  
Istituto Universitario di Studi Superiori (IUSS), V.le Lungo Ticino Sforzo 56, 27100 Pavia, Italy

## 1 Introduction

Italian seismic provisions and seismic zonation were updated several times during the last century. Therefore, a large portion of buildings has not been designed for an adequate level of seismic resistance required under modern design provisions. The majority of the Italian school buildings are especially vulnerable to seismic ground motion since they are judged to be seismically inadequate. An ad hoc seismic risk evaluation of the school buildings becomes therefore of fundamental importance for planning an accurate retrofitting of these buildings and for the safety of their occupants.

The seismic vulnerability evaluation of the school buildings is a topic that has been discussed by several authors in the last decades. For example the SAVE project-Task 2 [1] includes the vulnerability study of public and strategic buildings located in central and southern of Italy, while the “Scuola Sicura” project [2] provides the evaluation of the structural characteristics of school buildings located in the Molise district. Also EUCENTRE research groups [3, 4] have dealt with this topic proposing methods for seismic risk assessment of school buildings and then applying them to schools located in some Italian districts. Also, a seismic testing program [5] is in progress in accordance with Italian regulations (Article 2, paragraphs 2, 3 and 4 of [6]). According to this program, schools are classified as relevant buildings in relation to the consequences of a possible collapse. Therefore seismic controls are required, with priority given to the schools in seismic zone 1 and 2. Although this program [5] had originally set the time limit for testing to 2008, later extended to 2011, the controls are not yet complete even for zone 1 and 2.

Due to the lack of available data, the studies performed in recent years haven't affected all the schools throughout the country. The previous studies were not concerned with the school buildings located in districts with low seismic hazard. However the schools located in these areas may have high levels of vulnerability having been designed in the absence of seismic regulations and this could result in a high seismic risk.

To the authors' knowledge, the study presented herein is the first where the maps of conditional probability of damage and seismic risk are obtained at a national level, since it has been carried out considering most of the Italian school buildings. The available data refer to the survey of all school buildings (“Anagrafe Edilizia Scolastica”) carried out by the Ministry of Education (“MIUR”) to identify various safety-related parameters. The collected survey forms comprise about 70 % of the Italian school buildings, and contain data that allow to identify the geographical location of the building, as well as its structural characteristics (i.e., age, number of storeys, construction type, and preservation status), its security conditions and the features of rooms and sporting facilities.

## 2 Adopted Procedure

This research work describes the method proposed for identifying the most seismic vulnerable Italian school buildings and for assigning priorities for the execution

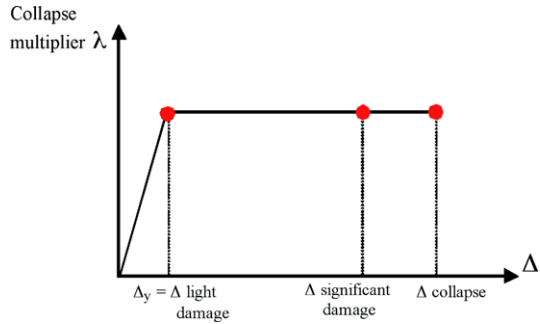
of detailed inspections and structural retrofitting measures. The adopted method is based on an initial proposal by Grant et al. [3]. It comprises multiple steps of assessment of increasing level of detail, each one substantially reducing the size of the building inventory since only the buildings most at seismic risk are considered. The procedure consists of two phases which correspond to the two levels of the available building information. In both phases, the seismic risk is defined considering the probability of reaching or exceeding given limit states by comparing the demand with the capacity in terms of displacements. The vulnerability of the school buildings is defined by computing their capacity curves (known, in the technical literature, as pushover curves). The mechanics-based methodology SP-BELA (Simplified Pushover-Based Earthquake Loss Assessment), developed for large-scale vulnerability assessment, is used for performing the simplified pushover curves [7, 8] of the analysed buildings. In the first phase of the assessment, the capacity is computed as a function of the number of storeys, structural vertical typology, and building age written in the questionnaires of the “Anagrafe Edilizia Scolastica”. Based on these data, the buildings are subdivided in classes and random populations of buildings can be generated for each building class using Monte Carlo simulation. For each randomly generated building, a simplified pushover analysis is carried out using SP-BELA (Fig. 1), leading to the definition of the displacement capacity, vibration period and viscous damping of an equivalent single degree of freedom system [7, 8].

The second phase of the procedure is based on the data collected, at Regional level, through the 2nd Level Forms [9–11] of GNDT (“Gruppo Nazionale per la Difesa dai Terremoti”). In this second phase, only masonry buildings are taken into account since the complete GNDT 2nd Level Form for reinforced concrete (RC) buildings were few and, therefore, not statistically significant, whereas they allow the calculation of the Conventional Resistance (“Resistenza Convenzionale”) for masonry buildings. The Conventional Resistance is the lateral strength of the weakest storey of the building divided by the structure seismic weight. Therefore, the difference with respect to the first phase of the procedure is that the resistance factor of the capacity curve is computed directly with the data available within the form of the reference school building and not computed for each random generated building stock representative of the reference school building class.

If the results of the seismic testing program [5] became available, it would be possible to increase the number of levels of detail.

Due to the incompleteness of the available database, the second phase of the procedure cannot be applied to the overall Italian school building stock. Therefore, the estimate of the reduction in size of the building inventory moving from the first to the second phase of the procedure cannot be carried out. The study described herein does not apply the prioritisation procedure as a whole, but represents its validation in order to identify some possible shortcomings that need improvements.

**Fig. 1** Capacity curve for elastic-perfectly-plastic structural behaviour [8]



## 2.1 Definition of the Building Capacity

The capacity is evaluated as a function of the number of storeys, the structural typology and the year of construction. For each building class identified on the basis of this information, a sample of 1000 buildings is created by means of a Monte Carlo generation. The sample size of 1000 is considered statistically representative since its increase does not affect the final results. For RC buildings the procedure includes a simulated design with the Allowable Stress Method as this was the design method prescribed by the law prior to [12].

For each building of the sample a simplified pushover analysis is carried out using the SP-BELA methodology that allows to calculate the properties of an equivalent single degree of freedom system, such as the displacement capacity  $\Delta$ , the equivalent period of vibration  $T$  and the equivalent viscous damping  $\xi$  for each limit state.

Three limit state (LS) conditions have been taken into account [13]:

- Light damage: the building can be used after the earthquake without the need for repair and/or strengthening;
- Significant damage: the building cannot be used after the earthquake without strengthening;
- Collapse: the building becomes unsafe for its occupants as it is no longer capable of sustaining any further lateral force or the gravity loads for which it has been designed.

The limit state conditions previously described can be related to specific prescriptions of Italian design code [12, 14]. In particular, the reference limit state conditions for RC buildings are defined in relation to the chord rotation. For masonry structures, the damage is usually related to interstorey drift capacity, and the limit conditions have been identified through the results of experimental tests as described in [8].

An elastic-perfectly-plastic behaviour of the structure is assumed (Fig. 1), which effectively means that, in order to define the pushover curve, only the displacement capacity  $\Delta$  corresponding to the three LS and the lowest collapse multiplier  $\lambda$  of all the considered mechanisms need to be defined. Multiplying  $\lambda$  by the structure seismic weight gives the lateral strength of the weakest storey of the building.

In the first phase, the collapse multiplier  $\lambda$  is calculated for each of the 1000 buildings of the sample on the basis of the formulations reported in [7] for reinforced concrete buildings and in [8] for masonry buildings. In the second phase, on the other hand, the collapse multiplier  $\lambda$  coincides with the Conventional Resistance calculated using the data included in the GNDT 2nd Level Form for masonry buildings.

In the first phase a building class is associated to each school belonging to the database of the “Anagrafe Edilizia Scolastica” and then, for each class, a sample of buildings is generated and, for each of them, a capacity curve with different collapse multiplier and limit displacements. In the second phase, however, a building class is still associated to each building in the GNDT database (defined exclusively as a function of the number of storeys) and for each class is generated a sample of buildings, but the capacity curves are characterised by the same collapse multiplier, which coincides with the Conventional Resistance calculated using the data collected in the GNDT 2nd Level Form for the examined building, and different limit displacements.

### 2.1.1 Defined Classes of Buildings

In the first phase of the methodology, 47 classes of buildings (Fig. 2) have been identified in the database of the “Anagrafe Edilizia Scolastica”, based on the number of storeys, the horizontal and vertical structural typology and the year of construction.

Masonry buildings have been divided into three vulnerability classes: A = high, B = average, C = low. The three classes have been identified on the basis of the intersection of the horizontal and vertical structural typology, using the correspondence shown in Table 1. This correlation is reported in [15] and it was developed by Braga et al. [16] on the basis of the Irpinia’80 data. When there was not enough information to assign the class using the available data, a default class B was assigned. The number of storeys considered for masonry buildings is from 1 to 5.

A different criterion has been applied for the RC buildings since they are subdivided in two main classes: RC buildings that have not been seismically designed and RC buildings seismically designed. Comparing the seismic zone to which the municipality has been assigned and the period of building construction, it is possible to identify if a school building has been or not designed according to seismic design provisions. For seismically designed buildings, the seismic zone of the municipality at the period of construction has to be taken into account since it can be used, together with the provisions of the design codes of the same period, for defining the value of the design lateral force as a percentage of the total building weight. Figure 2 refers to three seismic zones in Italy, since the fourth one [17], characterised by the lowest value of seismicity, has been disregarded because it was introduced by recent regulation and not really used to design buildings so far. In SP-BELA, the buildings are designed considering only gravity-load before seismic classification. Then, following the classification and depending on the seismic zone of the municipality, a base shear coefficient, included in the design of the buildings, was

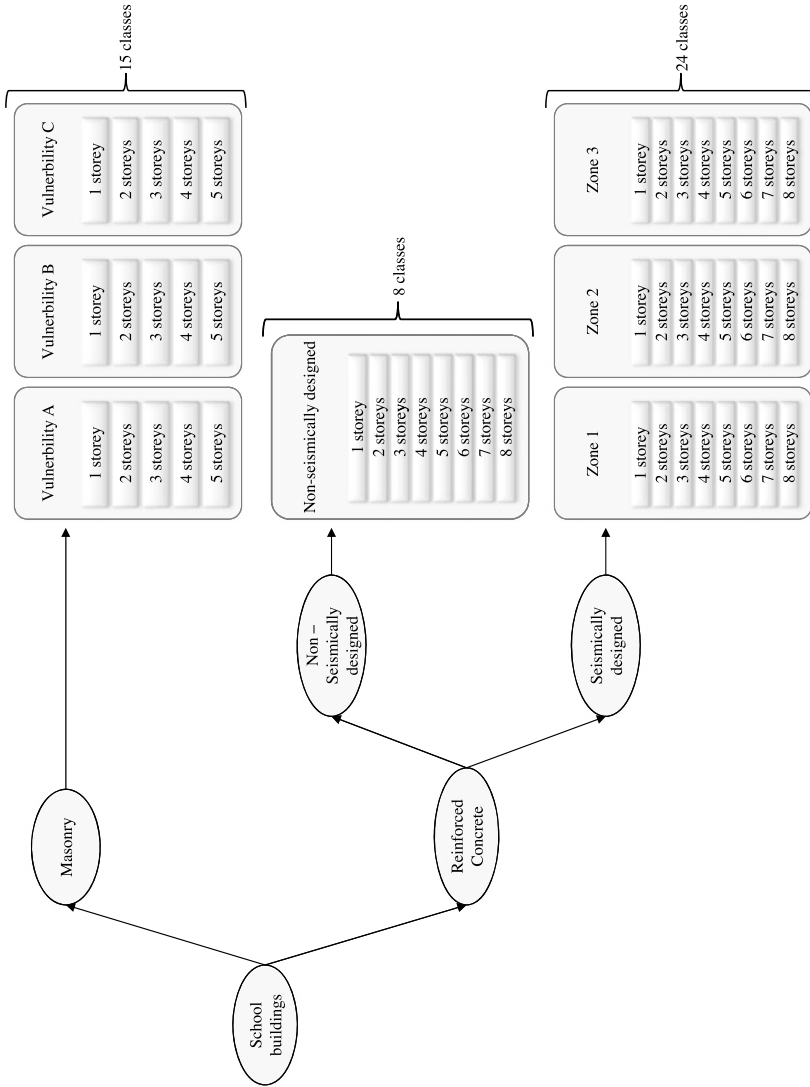


Fig. 2 Classes of buildings considered in the study

**Table 1** Vulnerability classes from horizontal and vertical structural type

Horizontal	Vertical		
	stone	tuff	brick
vault	A	A	A
wood	A	A	B
iron	B	B	C
CA	B	C	C

assigned. For buildings assigned to Zone 1, this coefficient has been taken as 10 % of the weight, for buildings in Zone 2 as 7 % and in Zone 3 as 4 %. The number of storeys considered for RC school buildings is: 1, 2, 3, 4, 5, 6, 7, more or equal to 8 (Fig. 2).

The second phase of the analysis has been developed for masonry buildings only. The classes of buildings considered in this phase are only 5, depending on the number of storeys. In this case, masonry buildings were not divided into vulnerability classes because the Conventional Resistance parameter already includes information about the building vulnerability.

### 2.1.2 Computed Fragility Curves

As explained in Sect. 2.1.1, in phase 1 the masonry buildings were divided into three vulnerability classes: class A, B and C. The SP-BELA method does not provide fragility curves for highly vulnerable masonry buildings due to the lack of the necessary data for the description of the sample, as the only statistically significant sample available was limited to good quality masonry buildings. Also the description of the building capacity through a pushover curve does not account for the local collapse mechanisms which are the most common collapse mechanism for highly vulnerable masonry buildings. To define the fragility of highly vulnerable masonry buildings a hybrid method was therefore adopted. SP-BELA was used to define the fragility of low vulnerability masonry buildings (class C). The curve obtained for buildings of type C was then modified by including data of observed damage from recent earthquakes to obtain the fragility curves for class A and B.

Observed damage data herein included are those summarised in the damage probability matrices (DPM) published in Braga et al. [16]. Such matrices come from a statistic of post-event data collected in the municipalities affected by the 1980 Irpinia earthquake. For the evaluation of these matrices, the buildings were classified in 3 vulnerability classes (A = high, B = average, C = low). The hazard is expressed in MSK macroseismic intensity scale [18]. The DPMs consider 5 damage levels, besides the absence of damage.

The first step was to find a correspondence between the levels of damage taken into account in the DPMs and the SP-BELA limit states. It was assumed that the

**Fig. 3** Fragility curves for limit state of significant damage obtained from DPM developed by Braga et al. [16] and lognormal function which best interpolates them

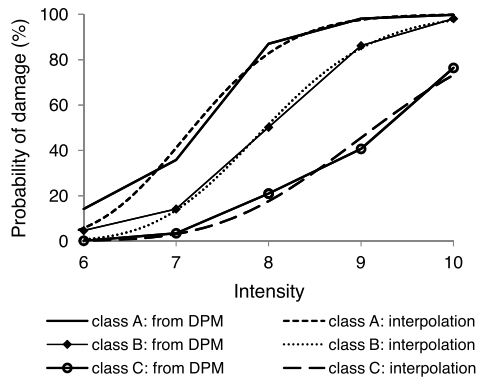


**Table 2** Multiplicative coefficients that allow to obtain, for each limit state, the fragility curves for the class A and B starting from the curve obtained for the class C

Limit state	Vulnerability class	
	A	B
Light damage	1.36	1.17
Significant damage	1.28	1.16
Collapse	1.26	1.15

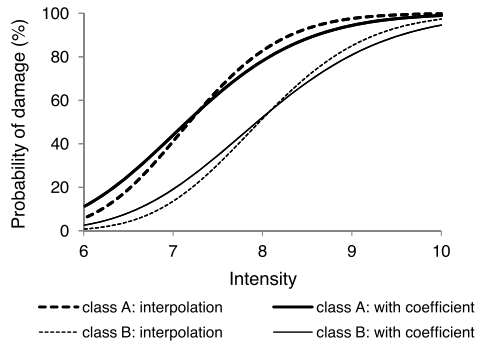
damage levels 1 and 2 correspond to light damage, the level 3 corresponds to significant damage and levels 4 and 5 correspond to collapse. The DPMs developed by Braga et al. [16] were used to understand the relationship in terms of probability of damage between the three classes of masonry. Fragility curves have been defined through the best fit with a lognormal curve of the points corresponding to the damage probability matrix. Hence, the authors have assumed that the fragility curves corresponding to the different vulnerability classes are characterised by a different mean value and by the same dispersion parameter (i.e. the same coefficient of variation, CV).

Figure 3 shows the curves for the limit state of significant damage. In the aforementioned figure, a continuous line is used for the curves resulting from the discrete DPMs developed by Braga et al. [16], while the dashed lines refer to the lognormal best fit curves. The good correspondence between the curves demonstrates that the lognormal distribution is a good mathematical function to describe the probability distribution of the damage data coming from observations.

For each limit state, the ratio between the mean value of the curve for class C and the mean of the curves for class A and B was calculated. These coefficients are reported in Table 2 as a function of the limit state. In order to validate the assumption that the CV does not change from one vulnerability class to the other, Fig. 4 shows the comparison between the fragility curves for classes A and B obtained by interpolating the corresponding DPM (dashed line) and the fragility curves obtained starting from the curve for class C and modifying the average value using the coefficients shown in Table 2 (continuous line) for the significant damage limit state. Plots obtained from the curve for class C show a good approximation with those derived



**Fig. 4** Fragility curves for limit state of significant damage obtained by interpolating the corresponding DPM of Braga et al. [16] and curves obtained with the calculated coefficients



by the interpolation of the DPMs. Therefore, SP-BELA fragility curves are calculated for the vulnerability class C and then those for classes A and B are obtained using the coefficients summarised in Table 2.

The fragility curves for the RC buildings were calculated only applying the mechanical method.

## 2.2 Conditional Probability of Damage

In SP-BELA the comparison between seismic capacity and demand is carried out in terms of displacement. The building displacement capacity has been introduced in Sect. 2.1. The seismic demand imposed by the earthquake to the structure is calculated with reference to the elastic spectrum related to the school building location, computed according to the formulation proposed in [12, 14]. This formulation has been obtained through least-square interpolation of the median acceleration spectrum derived from the probabilistic hazard study performed by DPC-INGV project [17] for a grid of points (each one at distance of 0.05 degrees) used for the whole country. The formula and the coefficients given by the Italian code [12, 14] allow the computation of the mean spectral accelerations for each point of the grid and for seismic events characterised by a return period ( $T_r$ ) of 30, 50, 72, 101, 140, 201, 475, 975 and 2475 years, respectively.

In this study, the least-square interpolation method has been applied to the median acceleration spectrum (50th percentile) plus and minus one standard deviation for deriving the parameters that allow the computation of the 84th and 16th percentile spectral accelerations, respectively. Therefore, the seismic demand imposed by the earthquake to the structure is computed with respect to the 16th, 50th and 84th percentile acceleration spectra. Bedrock conditions with no topographic amplification have been assumed for the Italian territory, since no data are available at present for the evaluation of the site conditions where the school buildings are located.

The seismic demand is derived from the elastic response spectrum knowing the location of the school building, for a given return period and a selected percentile

(16th, 50th, and 84th). From SP-BELA method, the vibration period  $T$  of the building and the equivalent viscous damping  $\xi$  are computed for each limit state. Knowing the response period, the spectral ordinate is directly derived for each LS. Knowing the equivalent viscous damping, the spectra reduction factor  $\eta$ , used to take into account the energy dissipation capacity of a given structure for a given LS, is then computed, as suggested for instance in [19]:

$$\eta = \sqrt{\frac{7}{2 + \xi}} \quad (2.1)$$

For RC frames, the equivalent viscous damping  $\xi$  in Eq. (2.1) has been obtained as a function of the ductility, using Eq. (2.2) [19]. For masonry buildings, the damping values suggested in [20] have been adopted (5 %, 10 % and 15 %, respectively) for each limit state.

$$\xi = 0.05 + 0.565 \left( \frac{\mu - 1}{\pi \mu} \right) \quad (2.2)$$

The displacement spectral ordinates are defined starting from the spectral accelerations:

$$S_d = S_a \left( \frac{T}{2\pi} \right)^2 \quad (2.3)$$

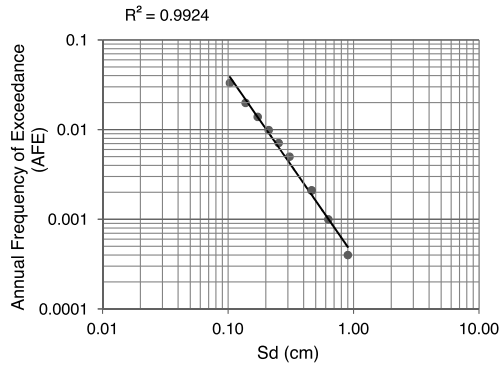
where  $S_d$  represents the displacement demand,  $S_a$  the acceleration demand and  $T$  the period of vibration of the building.

Based on the previously introduced ingredients, the conditional probability of damage, where the condition is that a given seismic event will occur, can be computed for the nine return periods  $T_r$  considered in the Italian seismic code [12]. Random populations of buildings are generated for each building class (1000 buildings for each one of the 47 classes shown in Fig. 2) using Monte Carlo simulation. The period of vibration  $T$ , the displacement capacity  $\Delta$  and the ductility factor  $\eta$  at the three different damage limit states (Fig. 1) can be calculated for each randomly generated building through a simplified pushover analysis performed using SP-BELA (Sect. 2.1). Knowing  $T$  at each LS and for a given overdamped (using Eq. (2.1)) displacement response spectrum, the displacement demand of a given building of the random population can be predicted and compared with its limit state displacement capacity. This procedure is repeated for the 1000 buildings randomly generated for each class of school buildings (Fig. 2). The sum of all buildings whose displacement capacity is lower than the displacement demand divided by the total number of buildings gives an estimation of the probability of exceeding a given limit state. The output of these computations is the conditional probability of damage, given the occurrence of a seismic event characterised by a given return period  $T_r$ .

### 2.3 Computation of the Seismic Risk

The seismic risk is computed knowing the hazard curve of the place where the school building is located. Such curve gives the probability of occurrence of a given

**Fig. 5** Relationship between the annual frequency of exceedance (AFE) and  $S_d$  ( $T = 0.2$  sec)



level of ground shaking severity in a specific exposure time  $t_d$ . Severity can be expressed in terms of the Annual Frequency of Exceedance (AFE), which is the reciprocal of the return period  $T_r$ . The hazard curve represents the relationship between AFE and a ground motion parameter, herein assumed as the spectral displacement  $S_d$ . The logarithm of the  $S_d$  and the logarithm of the corresponding AFE ( $= 1/T_r$ ) can be assumed to be linearly-related, at least for return periods of engineering interest. The gradient of the log-log hazard curve is named  $-k$ , according to the definition in Part 1 of the Eurocode 8 [21]. As an example, Fig. 5 plots the spectral ordinates  $S_d$  for a vibration period of 0.2 seconds. Since the values are linearly related, the hazard curve is defined knowing a value of  $S_d$  corresponding to a return period  $T_r$  and the slope  $k$  of the line interpolating all the other points and passing from a reference point.

The reference point is here conventionally assumed equal to the value at 475 year return period and the hazard curve is defined by the following relationship:

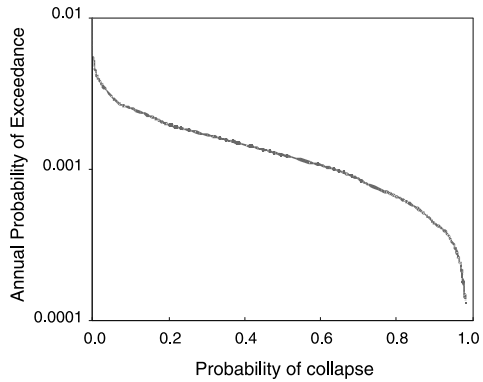
$$AFE = AFE_{475} \left( \frac{S_{d475}}{S_d} \right)^k \tag{2.4}$$

where  $AFE_{475}$  and  $S_{d475}$  are the annual frequency of exceedance and the spectral displacement corresponding to the 475 year return period, respectively.

Knowing the vibration period  $T$  of the structure, nine values of spectral accelerations  $S_a$  are computed in correspondence of the nine return periods  $T_r$  listed in [12]. Using Eq. (2.3), the  $S_a$  values are converted in spectral displacements  $S_d$ ; the next step is the derivation, in a log-log plane, of the line interpolating these points and passing for the point computed at a 475 year return period, and the slope  $k$  is finally calculated. Therefore, the hazard curve is directly derived and the displacement demand can be computed whatever return period is considered. It follows that all the events that could occur in a specific exposure time  $t_d$  can be taken into account. Hence, the seismic demand is then computed and compared with the capacity for each event, obtaining the conditional probability of exceeding a given limit state.

The seismic risk is the unconditional probability of failure the limit state conditions. For its computation, the hazard curve previously expressed as a function of the frequency has to be given in terms of probability. The occurrence of the events

**Fig. 6** Exceedance curve of the collapse limit state in an exposure time of 1 year, for a given class of buildings



is assumed to follow the Poisson process, that is a memoryless distribution such that each event occurs independently of one another. Therefore, the occurrence probability ( $q$ ) of an event with severity AFE, in the exposure time  $t_d$ , is given by the following equation:

$$q = 1 - e^{-t_d AFE} \tag{2.5}$$

Since AFE is related to the spectral displacement  $S_d$  according to Eq. (2.4), the probabilistic hazard curve can be expressed as a function of  $S_d$ :

$$q = 1 - e^{-t_d AFE_{475} (S_{d475}/S_d)^k} \tag{2.6}$$

Three exposure times  $t_d$  are taken into account in this study: 1 year, 10 years and 50 years. If, for example, the annual collapse risk has to be computed, the corresponding hazard curve is obtained from Eq. (2.6) with  $t_d = 1$ . The derived curve gives the annual probability of occurrence of an event with severity AFE expressed as a function of  $S_d$ . The hazard curve has to be related to the conditional probability of collapse, i.e. the vulnerability, where the condition is the occurrence of an event for a given return period  $T_r$ . Knowing that  $T_r$  can be expressed as a function of AFE and AFE is related to  $S_d$  according to Eq. (2.4), the conditional probability of damage is then obtained and the condition is expressed as a function of  $S_d$ . Therefore, since two curves are available—the hazard curve and the vulnerability curve—both expressed as a function of  $S_d$ , the exceedance curve of a given limit state in the exposure time  $t_d$  can be computed as a discrete function.

Shown in Fig. 6 is the exceedance curve for a exposure time  $t_d$  of 1 year and the collapse limit state. The annual seismic risk is given by the analytical integration of this curve, using the following equation:

$$\text{Seismic Risk} = \sum_{i=0}^{+\infty} \left[ \frac{APE_{2(i+1)} - APE_{2i}}{6} \right] \cdot [P_{\text{collapse}_{2i}} + 4P_{\text{collapse}_{2(i+0.5)}} + P_{\text{collapse}_{2(i+1)}}] \tag{2.7}$$

where APE is the Annual Probability of Exceedance, and  $P_{\text{collapse}}$  the probability of collapse.

If the exposure time  $t_d$  is different from 1 year, the ordinates of the derived plot are the probability of exceedance in the considered  $t_d$ .

### 3 Available Databases

The procedure described for the evaluation of the seismic risk has been applied for processing the data of two databases: the survey forms of the “Anagrafe Edilizia Scolastica” (used in the first phase of the procedure) and the GNDT 2nd Level forms (used in the second phase of the procedure). The school buildings of the “Anagrafe Edilizia Scolastica” forms have been georeferenced based on the street address. Then, a correspondence between these buildings and the ones of the GNDT forms has been derived in order to compare the two sets of data. Since there is no a common identification to be associated to the school buildings of the two databases, the correspondence has been carried out using the geographical location. The georeferenced buildings belonging to the “Anagrafe Edilizia Scolastica” database are 49503, whereas the ones belonging to the GNDT database and with a correspondence in the first database are 3553.

#### 3.1 School Buildings Analysed in the First Phase of the Procedure

As previously introduced in Fig. 2, the school buildings of the “Anagrafe Edilizia Scolastica” database have been subdivided in 47 classes. However, there are 17328 buildings of this database without the specification of their structural typology or the number of storeys. Therefore, the latter could not be introduced in one of the classes of Fig. 2. Hence, some assumptions have been done in order to automatically assign the needed information for classifying these school buildings. Furthermore, additional hypotheses have been required for assigning one of the two main structural typologies considered in this study (masonry and reinforced concrete) to those buildings with a mixed typology. The “reinforced concrete and masonry” or “masonry and other typology” structures have been analysed as masonry buildings, whereas the “reinforced concrete and other typology” structures have been classified as “reinforced concrete” buildings. With these assumptions, it was possible to include 7211 buildings belonging to the 17328 buildings without clear specifications. Therefore, there are 10117 school buildings of the “Anagrafe Edilizia Scolastica” database that cannot be analysed since there are no enough information for assigning a structural typology or because their assigned structural typology in the forms was “other”. Starting from the available 49503 school buildings of the “Anagrafe Edilizia Scolastica” database, the buildings analysed in the first phase of the procedure are 39386, subdivided in 19749 masonry structures and 19637 RC structures.

Figure 7a shows the map with the location of the 49503 georeferenced school buildings of the “Anagrafe Edilizia Scolastica” database, and Fig. 7b shows a bar

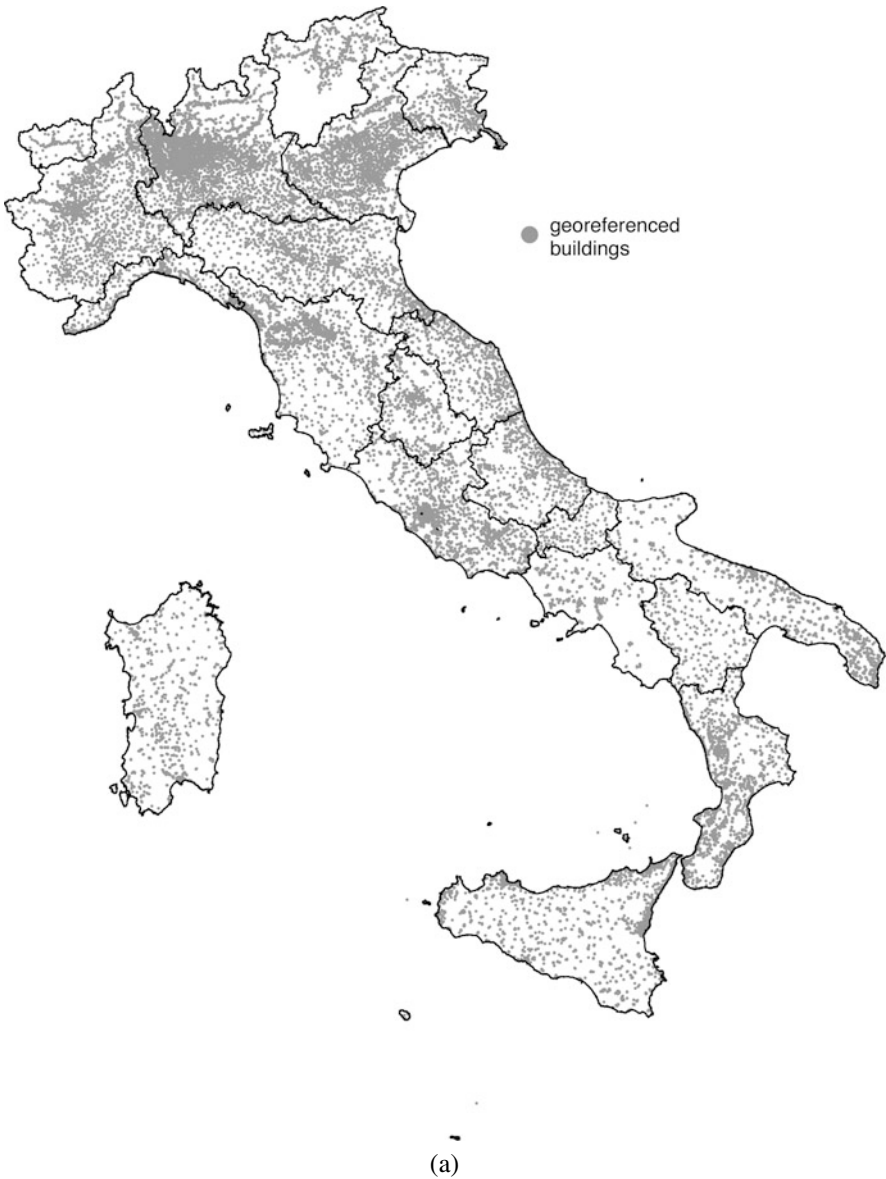


**Fig. 7** Georeferenced school buildings (a) and their classification as a function of their structural typology (b)

chart with the numbers of buildings considered (additionally subdivided according to their structural typology) or omitted in the proposed procedure.

Figure 8 shows the distribution of buildings based on the number of storeys: almost half of all investigated school buildings are two storey structures and more than 90 % of the buildings has a number of storeys less than four.

Fig. 7 (Continued)

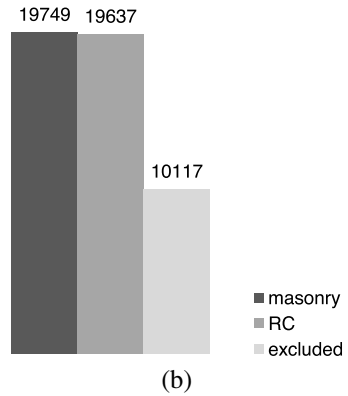


Fig. 8 Distribution of school buildings based on the number of storeys

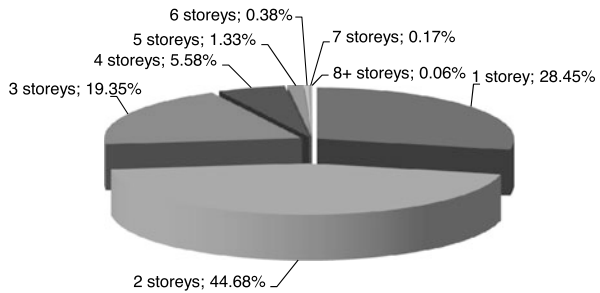


Fig. 9 Distribution of buildings according to the degree of education and the structural typology

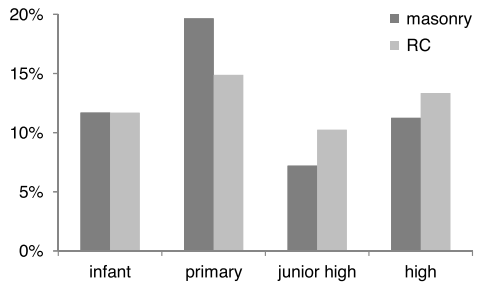
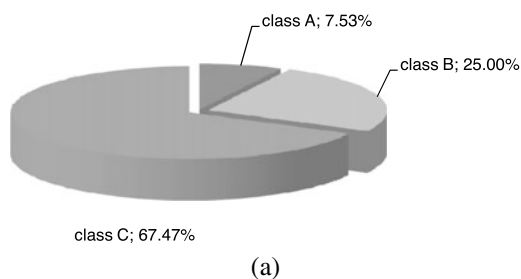


Figure 9 shows the distribution of buildings according to the degree of education and the structural typology. Primary school buildings are probably the older structures and this can justify that the majority of them has a masonry structural typology. On the contrary, the junior high and high school buildings, more recently built, are mostly in RC.

As explained in Sect. 2.1.1, masonry buildings have been divided into classes of vulnerability A, B and C as a function of horizontal and vertical structural typology. Figure 10a shows the distribution in the three vulnerability classes of 19749 masonry buildings considered in the analysis, while the map reported in Fig. 10b shows, for each district, the number of masonry school buildings in class A, B and

**Fig. 10** Division into vulnerability classes for masonry school buildings in percentage (a) and in number of building for each district (b)



C, respectively. More than 60 % of the buildings is in class C, the best class. In fact school buildings have always been considered “relevant” structures and were designed with greater attention to design details.

### 3.2 School Buildings Analysed in the Second Phase of the Procedure

The school buildings of the GNDT database whose data of the 2nd Level forms allow the calculation of the Conventional Resistance and with a correspondence in the “Anagrafe Edilizia Scolastica” database are 3553. However, five of these masonry buildings cannot be analysed since the data of the compiled survey forms are not coherent. Therefore, the school buildings considered in the second phase of the methodology are 3548, divided in five classes according to the number of storeys (Table 3).

The map shown in Fig. 11a gives the location of the school buildings analysed in the second phase of the methodology. In addition, Fig. 11b shows the distribution of such buildings for the different seismic zones (from 1 to 3). It has to be pointed out that there are no school buildings belonging to seismic zone 4 (characterised by the smallest seismic hazard) since the compilation of the GNDT 2nd Level forms has been carried out only for the buildings located in zones with medium-high seismicity.

**Table 3** Masonry school buildings analysed in the second phase of the procedure

No. of storeys	No. of buildings
1 storey	785
2 storeys	1215
3 storeys	1156
4 storeys	356
5 storeys	36



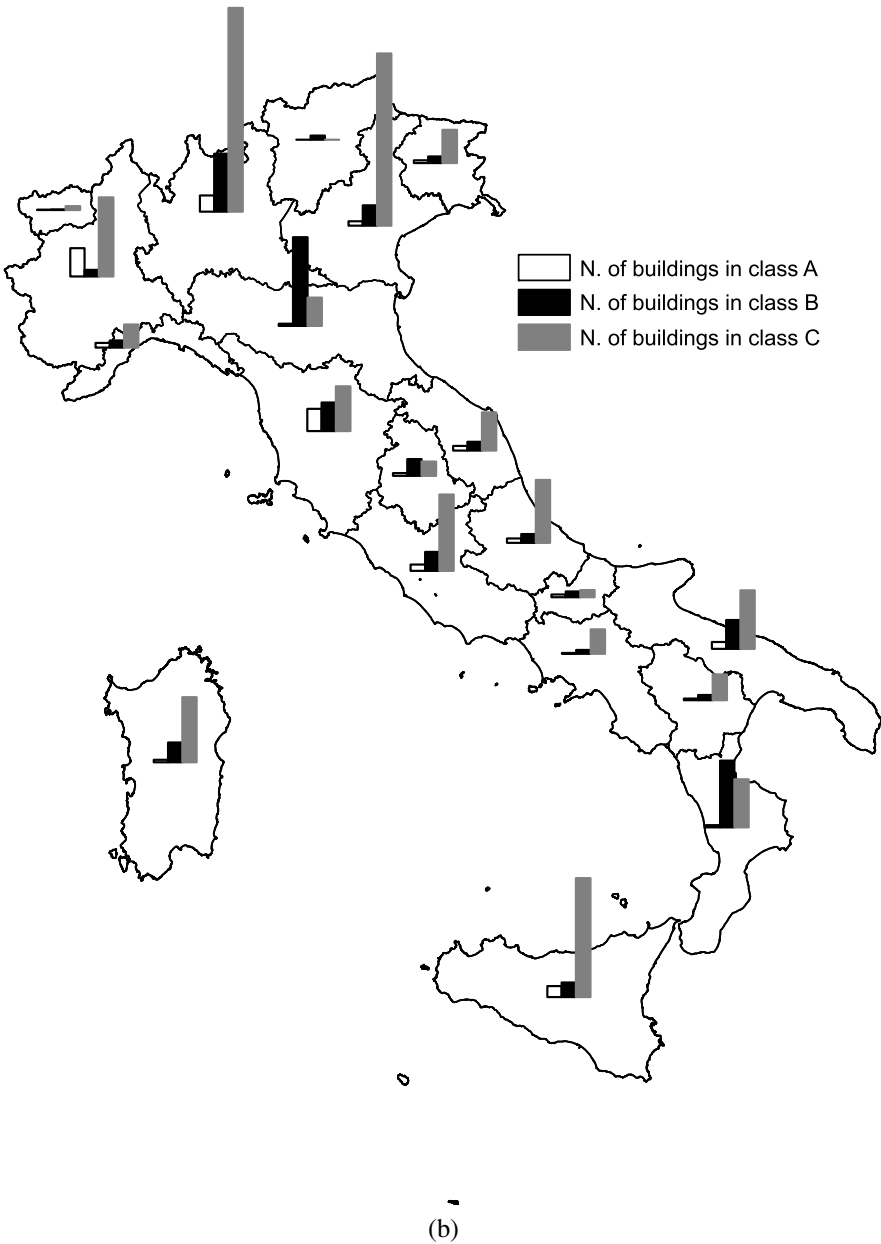
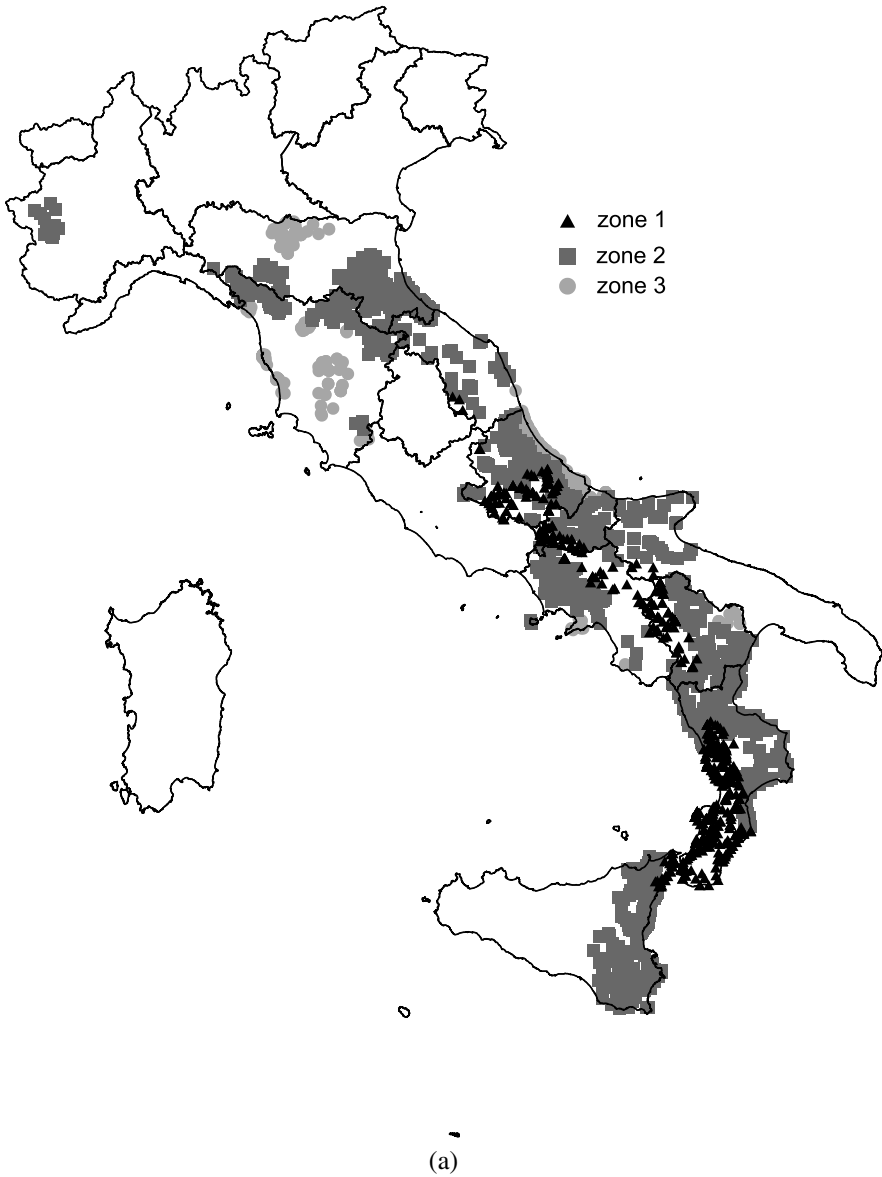


Fig. 10 (Continued)

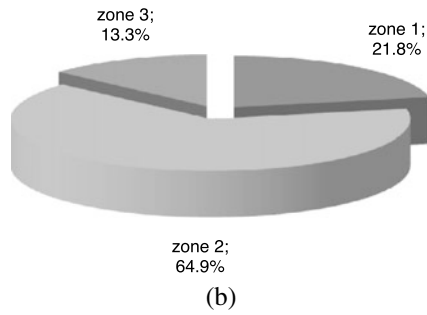
The Conventional Resistance has been computed for each one of the 3548 school buildings previously described. Knowing this value and its correspondence with the



**Fig. 11** School buildings analysed in the second phase of the procedure (a) and organised by seismic zone (b)

collapse multiplier  $\lambda$  (as anticipated in Sect. 2.1), the plateaux of the simplified capacity curve is automatically defined for each one of the analysed masonry school buildings.

**Fig. 11** (Continued)



## 4 Discussion of the Results

In this chapter are presented the results obtained in terms of conditional and unconditional probability of damage for the three limit states considered (light damage, significant damage and collapse).

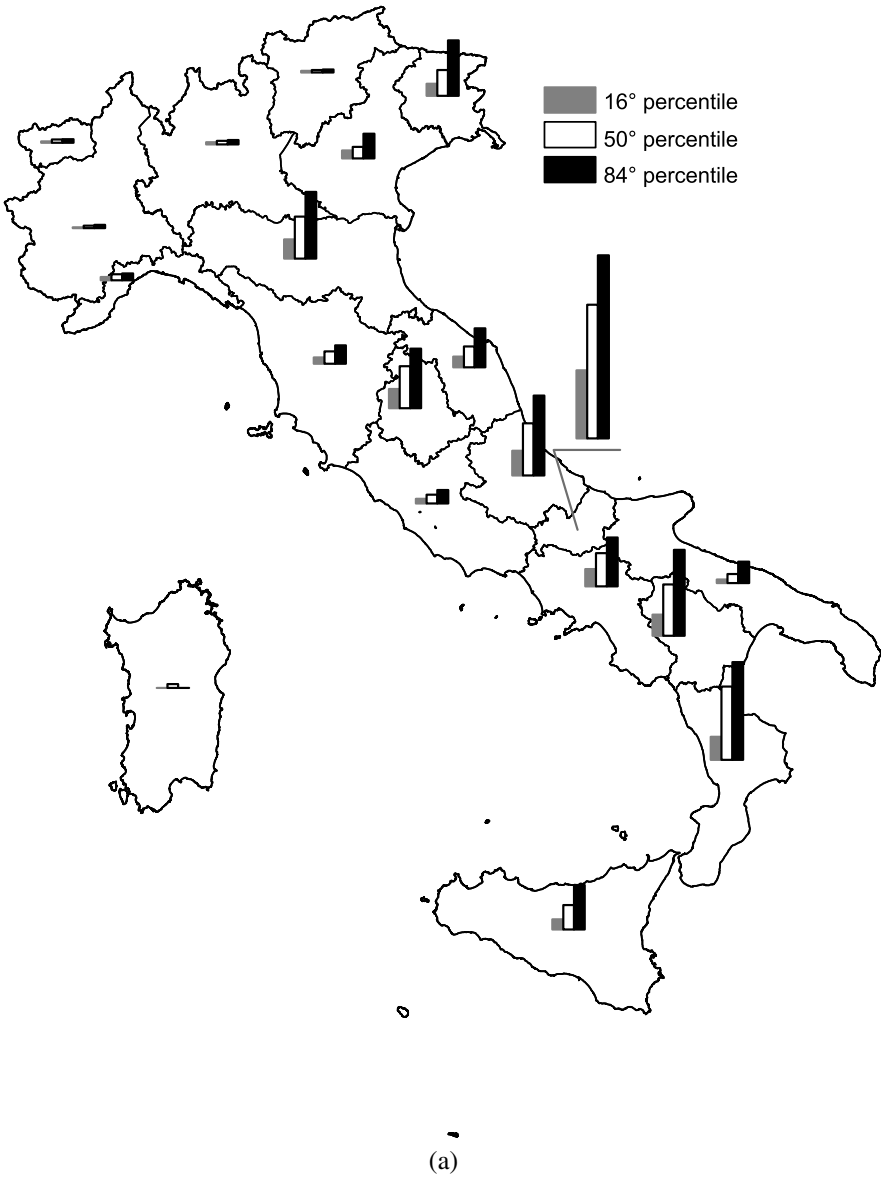
### 4.1 Results of the First Phase of Analysis

Figure 12a shows the conditional probability of exceeding the significant limit state for a seismic event with a 475 year return period, computed with respect to the 16th, 50th and 84th percentile acceleration spectra. The map reported in Fig. 12b shows the unconditional probability of exceeding the significant limit state calculated for three exposure times (1 years, 10 years, 50 years). This is an “unconditional” probability of damage, because it was considered the hazard curve associated with each school building, i.e. the probability that occurs a specific ground shaking in a given exposure time. The “conditional” probability of damage is a point on the fragility curve, while the “unconditional” probability derived from the integration of this curve with the hazard curve.

Masonry is the structural typology that mainly affects the results because it is very popular in Italy, even in areas of high seismicity, and masonry buildings are the most vulnerable structures. Figure 13 shows the influence of structural typology on the mean probability of damage. The mean overall value is close to the mean value for masonry buildings, particularly in districts with the highest values, while, for the districts with lower probability of damage, the mean value is equidistant from the mean values for the masonry and the RC buildings.

### 4.2 Correlation Between the Results Obtained in the Two Phases of the Procedure

The correlation between the results obtained in the two phases of the procedure for the 3548 masonry school buildings is plotted in Fig. 14 in terms of seismic risk for an exposure time of 50 years.



**Fig. 12** Mean value for each district of the: conditional probability of exceeding the significant limit state for a 475 year return period (a) and the unconditional probability of exceeding the significant limit state (b)

Figure 14 shows that the correlation between the results of the two phases of the procedure is quite satisfactory. The points over the line of best fit represent an underestimation of the seismic risk in the first phase of the analysis. This finding could

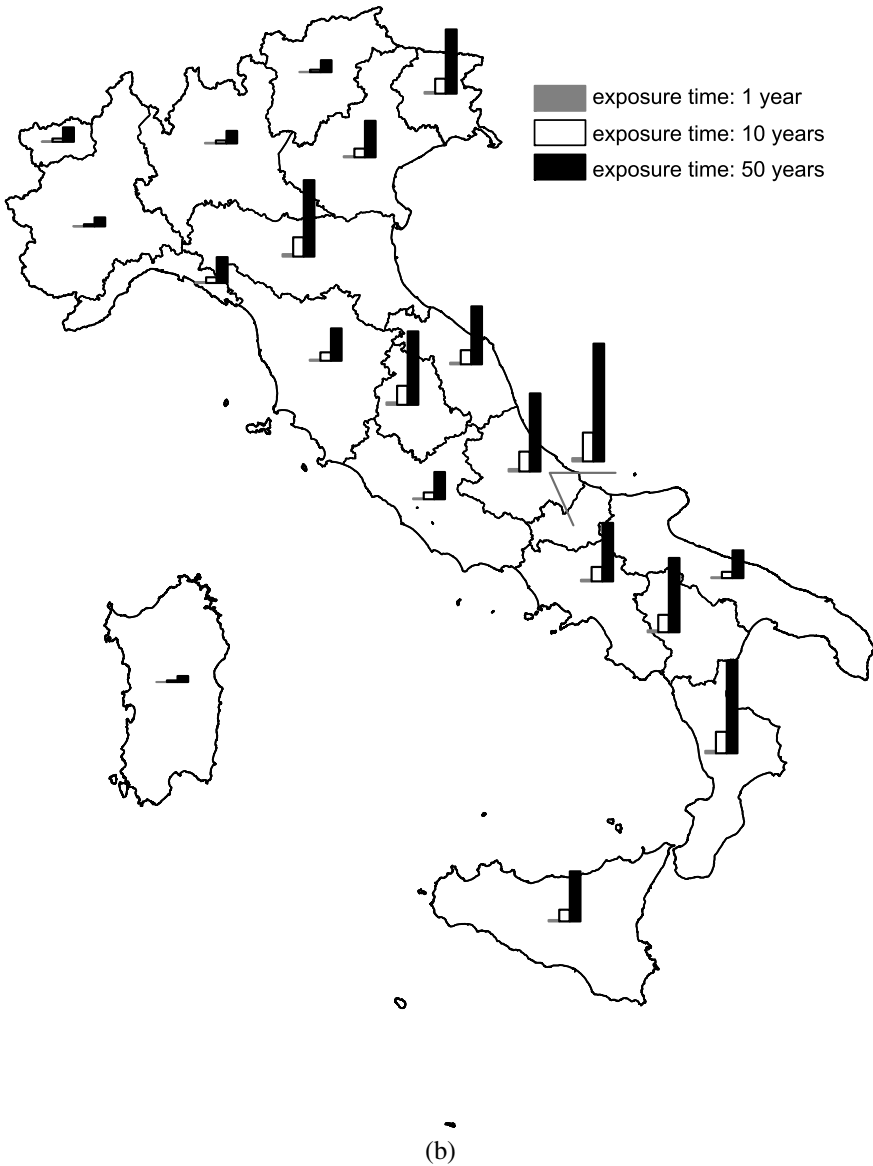
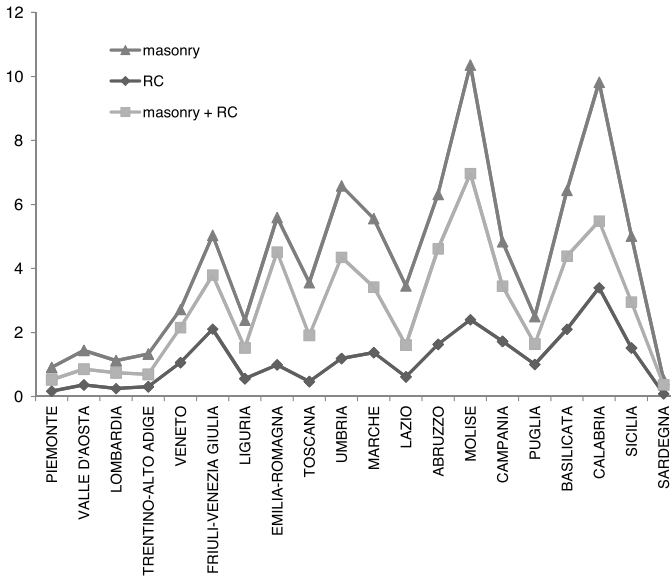


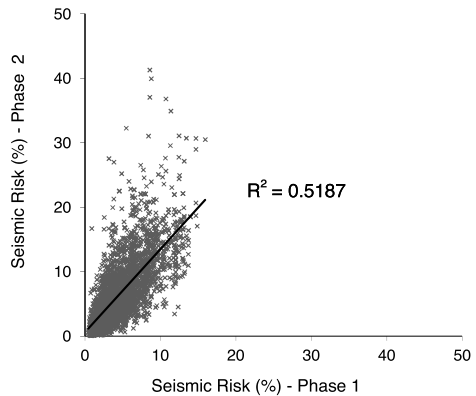
Fig. 12 (Continued)

be due to the different evaluation of the seismic vulnerability of the masonry structures. In the first phase of the procedure, SP-BELA fragility curves are calculated for the vulnerability class C and then those for classes A and B are obtained using the correction coefficients. In the second phase of the procedure, the Conventional Resistance is computed from the data of the survey forms and this resistance could



**Fig. 13** Mean value for each district of the unconditional probability of exceeding the significant damage limit state for an exposure time of 50 years

**Fig. 14** Correlation between the results obtained from the two phases of the proposed procedure

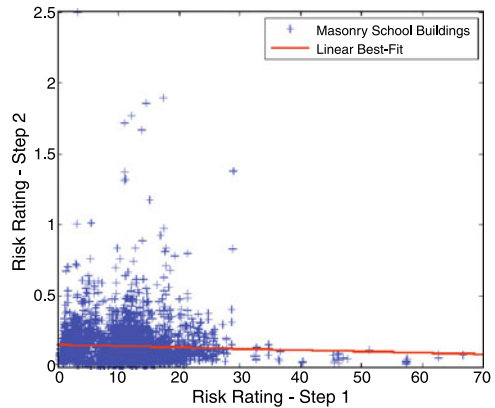


be less than the one assumed in the first phase of the procedure, leading to more vulnerable buildings.

The correlation shown in Fig. 14 is compared with that obtained from [4] for masonry buildings (Fig. 15) in the application of the multiphase methodology proposed in [3]. In the study enveloped by [4], it was used the information contained in the GNDT 1st and 2nd Level forms for schools located in central southern Italy.

Also in this case the methodology adopted is a multiphase procedure that includes two phases with increasing level of detail, where at each step the Risk Rating was calculated. The latter represents the relationship between seismic demand and

**Fig. 15** Risk Rating for step 1 and for step 2 [4]



capacity. The comparison between Fig. 14 and Fig. 15 shows that the methodology proposed in this study improves the correlation between the results obtained in the two phases of analysis.

## 5 WebGIS

Within this study a WebGIS platform that allows, by means of interactive maps and table, to locate the Italian school buildings, to view the data collected into the database of the “Anagrafe Edilizia Scolastica” and the information related to the seismic input, has been developed.

The developed processing of data can be viewed both with a desktop GIS and with a website GIS. It was decided to produce a WebGIS platform for several reasons: it can be accessed from various Internet stations, is multi-platform i.e. its functionality does not depend on the operating system used and, finally, all users will share the server upgrade since all data and functions are centralised in a server.

In Fig. 16 is shown an example of a map in which all the Italian school buildings are localised. In addition there are two charts about the elastic spectrum and the fragility curve related to the selected school building.

The developed WebGIS allows the following operations using the tools dedicated: find a school building by own geographical attributes (district, province and municipality), choose which layer display on the map, thematise the selected layer and add a new geographical layer related to the risk analysis selected. It is possible to perform “real time” scenario analysis too, as it will be discussed in the following section.

## 6 “Real Time” Damage Scenario

The routines developed for the calculation of the seismic risk give the possibility of calculating real-time damage scenarios, using the seismic input obtained from

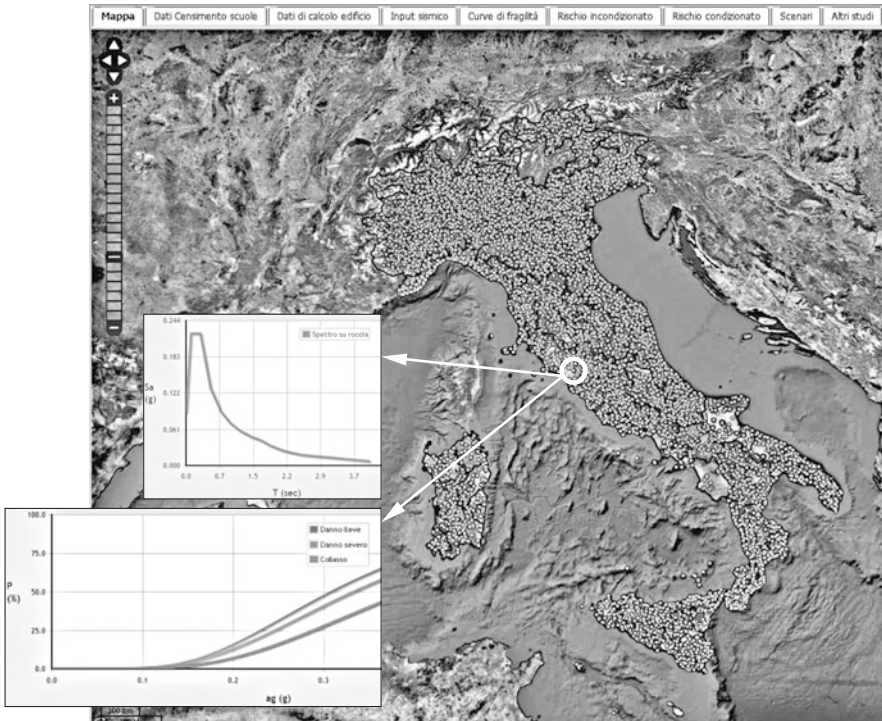


**Fig. 16** Localisation of school buildings on WebGIS, spectrum and fragility curve

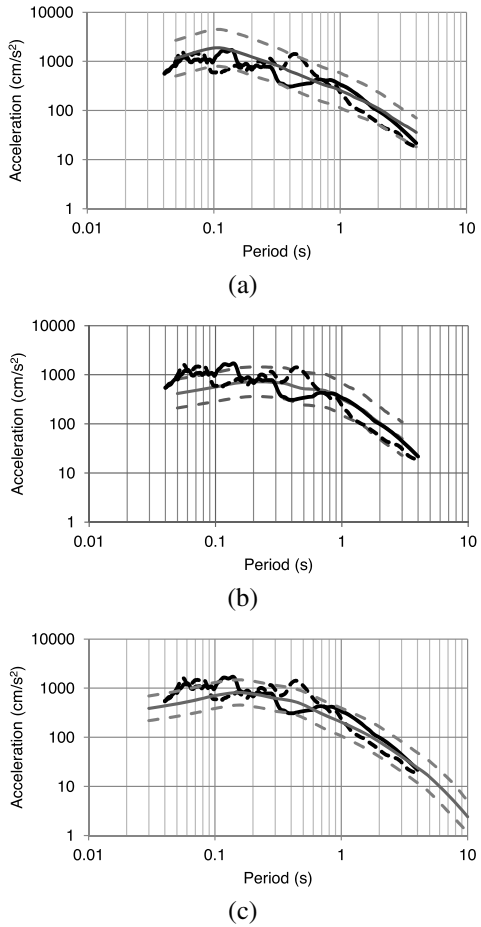
a selected attenuation law for a given magnitude and distance. Three attenuation relationships were selected among the most recent published in literature. Important requirements that have led to the selection were: (1) a simple form, which allows to generate a damage scenario with few input data, (2) estimate of spectral ordinates in terms of displacement or acceleration applied to both the high and low frequency, (3) good performance in terms of comparison with the spectra derived from the records of several real Italian earthquakes. The chosen laws are [22–24].

Figure 17 shows a comparison between the adopted attenuation laws and a record of the 2009 Abruzzo earthquake. The record comes from the ITACA database [25].

For the definition of the displacement spectrum which represents the demand imposed by the earthquake to the building, it is necessary to indicate, in addition to the attenuation law, the characteristics of the earthquake, such as magnitude, coordinates of the epicentre and the fault mechanism. The user must then indicate the radius within which the damage scenario has to be computed. Finally, the user must indicate the level of damage and the percentile of interest. Each created layer allows to view, on the map of Italy, the effect of the damage scenario selected for the school buildings located within the area indicated (Fig. 18).



**Fig. 17** Comparison between the attenuation law [22] (a), [23] (b) and [24] (c) and the record of the 2009 Abruzzo earthquake (E-W in *bold black* and N-S in *black dashed*) of the station AQA, Mw 6.3, epicentral distance 4.6 km [25]. In *grey* the attenuation law (*dashed line* for plus or minus standard deviation)



## 7 Closure

The novelty of this research study is represented by the maps of seismic risk for school buildings at a national scale. These maps give an overall view for the definition of a prioritisation procedure for surveys and detailed structural retrofitting measures.

A multiphase procedure has been proposed for the evaluation of the amount of school buildings requiring additional investigations. The methodology implements two analysis phases with an increasing level of detail such that the number of buildings analysed decreases at each step since only the buildings most at risk are considered.

The generation of seismic risk maps at a national scale is an outcome of the first phase of the proposed procedure. The data used for the map generation are based on the collected survey forms of the 70 % of the Italian school buildings. However, a reduced number of school buildings (3500) was available during the second phase

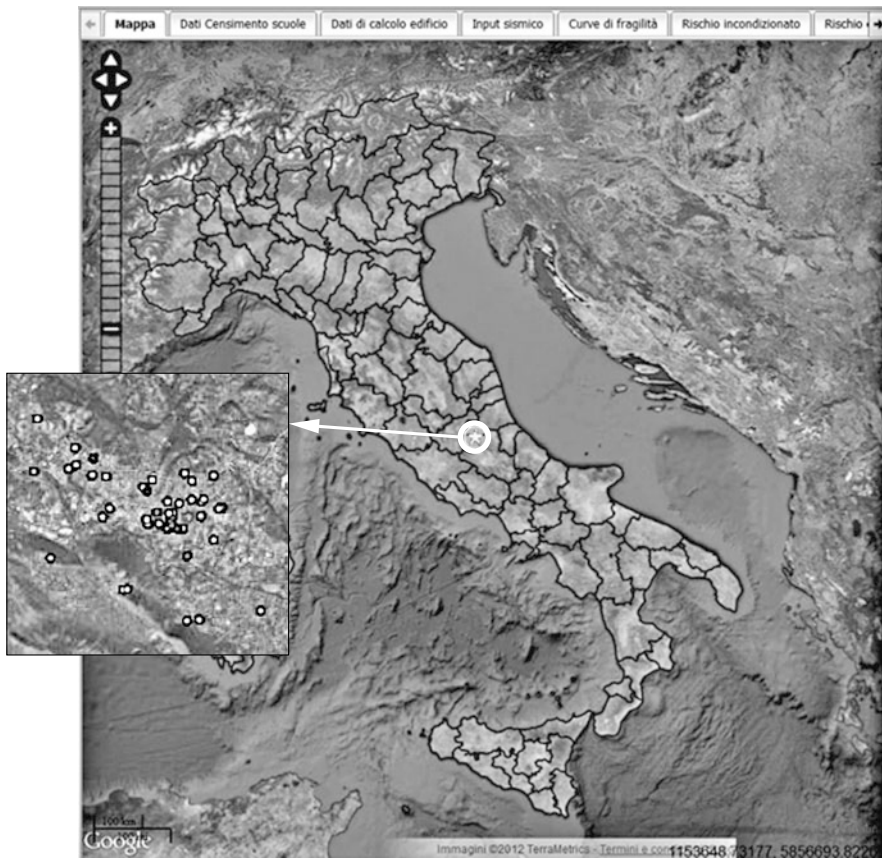


**Fig. 18** Example of a damage scenario

of the procedure. In fact, additional information on the building resistance should be collected and used during this analysis phase. In this study, this information was available for the school buildings of some districts of Italy and for masonry structures only.

The analyses were implemented in a specifically developed WebGIS platform that allows, through maps and tables, to view information and perform routine calculations. Moreover, the tool developed can provide significant assistance for emergency management in the immediate post-earthquake because it is able to perform an assessment of the real-time damage scenario.

Further developments of the proposed methodology are still required. It should be extremely useful to complete the collection of the data related to the school building resistance in all Italian districts and for all the structural typologies in order to allow a more accurate estimate of the seismic vulnerability of these buildings. This will allow the application of the second phase of the procedure at a national scale.

Therefore, it would be possible to apply the proposed procedure for the identification of the school buildings requiring priority of intervention.

**Acknowledgements** The study presented has benefited from financial support of the Prime Minister's Office—Department of Civil Protection; this publication, however, does not necessarily reflect the views and official policies of the Department. The authors would like to thank the support of the Italian Ministry of Research and Higher Education (MIUR—Ministero dell'Università e della Ricerca) for the availability of the “Anagrafe Edilizia Scolastica” forms. In closing, the authors are very grateful to Ms Miriam Colombi for the support related to the previously published works on the same topic, Ms Antonella Di Meo for finding the correspondence between the “Anagrafe Edilizia Scolastica” forms and the GNDT 2nd Level forms and Mr Marco Pagano for georeferencing the school buildings.

## References

1. Dolce M, Martinelli A (2005) *Inventario e vulnerabilità degli edifici pubblici e strategici dell'Italia centro-meridionale*, vol II, *Analisi di vulnerabilità e rischio sismico*. INGV/GNDT—Istituto Nazionale di Geofisica e Vulcanologia/Gruppo Nazionale per la Difesa dai Terremoti, L'Aquila
2. Dolce M, Masi A, Moroni C, Martinelli A, Mannella A, Milano L, Lemme A, Miozzi C (2007) *Sisma Molise 2002. Il progetto “Scuola sicura”: dall'indagine di vulnerabilità sismica alla esecuzione degli interventi*. Atti del XII convegno l'ingegneria sismica in Italia, Pisa
3. Grant DN, Bommer JJ, Pinho R, Calvi GM, Goretti A, Meroni F (2007) A prioritization scheme for seismic intervention in school buildings in Italy. *Earthq Spectra* 23(2):291–314
4. Crowley H, Colombi M, Calvi GM, Pinho R, Meroni F, Cassera A (2008) Application of a prioritization scheme for seismic intervention in schools buildings in Italy. In: *Proceedings of the 14th world conference on earthquake engineering*, Beijing
5. DPCM 21.10.2003 (2003) Disposizioni attuative dell'art. 2, commi 2, 3 e 4 dell'ordinanza del Presidente del Consiglio dei Ministri n3274 del 20 marzo 2003, recante «Primi elementi in materia di criteri generali per la classificazione sismica del territorio nazionale e di normative tecniche per le costruzioni in zona sismica». Dipartimento della Protezione Civile, GU 29.10.2003 n252
6. OPCM 20.03.2003 n3274 (2003) Primi elementi in materia di criteri generali per la classificazione sismica del territorio nazionale e di normative tecniche per le costruzioni in zona sismica. GU 08.05.2003 n105
7. Borzi B, Pinho R, Crowley H (2008) Simplified pushover-based vulnerability analysis for large scale assessment of RC buildings. *Eng Struct* 30(3):804–820
8. Borzi B, Crowley H, Pinho R (2008) Simplified pushover-based earthquake loss assessment (SP-BELA) method for masonry buildings. *Int J Archit Herit* 2(4):353–376
9. AA VV (1999) *Censimento di vulnerabilità degli edifici pubblici, strategici e speciali nelle regioni Abruzzo, Basilicata, Calabria, Campania, Molise, Puglia e Sicilia*. Dipartimento della Protezione Civile, Roma
10. AA VV (2000) *Censimento di vulnerabilità a campione dell'edilizia corrente dei centri abitati, nelle regioni Abruzzo, Basilicata, Calabria, Campania, Molise, Puglia e Sicilia*. Dipartimento della Protezione Civile, Roma
11. Zonno G coord (1999) *Rapporto finale CNR-IRRS alla Commissione Europea*. Contratto ENV4-CT96-0279, pp 95–102
12. DM 14.01.2008 (2008) *Approvazione delle nuove norme tecniche per le costruzioni*. GU 04.02.2008 n29
13. Calvi GM (1999) A displacement-based approach for vulnerability evaluation of classes of buildings. *J Earthq Eng* 3(3):411–438

14. Circolare applicativa delle NTC08 (2009) Circolare del Ministero delle Infrastrutture e dei Trasporti 2 febbraio 2009, n617 recante istruzioni per l'applicazione delle nuove norme tecniche per le costruzioni di cui al decreto ministeriale 14 gennaio 2008. Suppl ord n27 alla GU 26.2.2009 n47
15. Angeletti P, Baratta A, Bernardini A, Cecotti C, Cherubini A, Colozza R, Decanini L, Diotallevi P, Di Pasquale G, Dolce M, Goretti A, Lucantoni A, Martinelli A, Molin D, Orsini G, Papa F, Petrini V, Riuscetti M, Zuccaro G (2002) Valutazione e riduzione della vulnerabilità sismica degli edifici, con particolare riferimento a quelli strategici per la protezione civile. Rapporto finale Dipartimento della Protezione Civile—Ufficio Servizio Sismico Nazionale, Roma
16. Braga F, Dolce M, Liberatore D (1982) Southern Italy November 23, 1980 earthquake: a statistical study on damaged buildings and an ensuing review of the M.S.K.—76 scale. CNR-PFG n503, Rome
17. INGV-DPC S1 (2007) Proseguimento della assistenza al DPC per il completamento e la gestione della mappa di pericolosità sismica prevista dall'ordinanza PCM 3274 e progettazione di ulteriori sviluppi. <http://esse1.mi.ingv.it>
18. Medvedev AV, Sponheuer W (1969) Scale of seismic intensity. In: Proceedings of the 4th world conference on earthquake engineering, Santiago de Chile
19. Priestley MJN, Calvi GM, Kowalsky MJ (2007) Displacement-based seismic design of structures. IUSS Press, Pavia
20. Restrepo-Vélez LF, Magenes G (2004) Simplified procedure for the seismic risk assessment of unreinforced masonry buildings. In: Proceedings of the 13th world conference on earthquake engineering, Vancouver
21. Eurocode 8 (2004) Design of structures for earthquake resistance—part 1: General rules, seismic actions and rules for buildings. EN 1998-1:2004, Comité Européen de Normalisation, Brussels
22. Cauzzi C, Faccioli E (2008) Broadband (0.05 to 20 s) prediction of displacement response spectra based on worldwide digital records. *J Seismol* 12(4):453–475
23. Akkar S, Bommer JJ (2010) Empirical equations for the prediction of PGA, PGV, and spectral accelerations in Europe, the Mediterranean region, and the Middle East. *Seismol Res Lett* 81(2):195–206
24. Boore DM, Atkinson GM (2008) Ground motion prediction equations for the average horizontal component of PGA, PGV, and 5%-damped PSA at spectral periods between 0.01 and 10.0 s. *Earthq Spectra* 24:99–138
25. ITACA—ITalian ACcelerometric Archive. <http://itaca.mi.ingv.it/ItacaNet/>